Determination of Potassium Abundances
for Giant and Dwarf Stars in the Galactic Disk

Yoichi Takeda [1,2]

[1]*National Astronomical Observatory, 2-21-1 Osawa, Mitaka, Tokyo 181-8588, Japan*
takeda.yoichi@nao.ac.jp
[2]*SOKENDAI, The Graduate University for Advanced Studies, 2-21-1 Osawa, Mitaka, Tokyo 181-8588, Japan*

Abstract

An extensive study on the potassium abundances of late-type stars was carried out by applying the non-LTE spectrum-fitting analysis to the K I resonance line at 7698.96 Å to a large sample of 160 FGK dwarfs and 328 late-G /early-K giants (including 89 giants in the *Kepler* field with seismologically known ages) belonging to the disk population ($-1 \lesssim$ [Fe/H] $\lesssim 0.5$), which may provide important observational constraint on the nucleosynthesis history of K in the galactic disk. Special attention was paid to clarifying the observed behaviors of [K/Fe] in terms of [Fe/H] along with stellar age, and to checking whether giants and dwarfs yield consistent results with each other. The following results were obtained. (1) A slightly increasing tendency of [K/Fe] with a decrease in [Fe/H] (d[K/Fe]/d[Fe/H] ~ -0.1 to -0.15; a shallower slope than reported by previous studies) was confirmed for FGK dwarfs, though thick-disk stars tend to show larger [K/Fe] deviating from this gradient. (2) Almost similar characteristics were observed also for apparently bright field giants locating in the solar neighborhood (such as dwarfs). (3) However, the [K/Fe] vs. [Fe/H] relation for more distant *Kepler* giants shows larger scatter and is systematically higher (by $\lesssim 0.1$ dex) than that of dwarfs, implying that chemical evolution of K is rather diversified depending on the position in the Galaxy. (4) Regarding the age-dependence, a marginal trend of increasing [K/Fe] with age is recognized for dwarfs, while any systematic tendency is not observed for *Kepler* giants. These consequences may suggest that evolution of [K/Fe] with time in the galactic disk does exist but proceeded more gradually than previously thought, and its condition is appreciably location-dependent.

Key words: Galaxy: disk — Galaxy: evolution — stars: abundances — stars: atmospheres — stars: late-type

1. Introduction

While our understanding on the nucleosynthesis history of various elements in the Galaxy has remarkably grown thanks to accumulated observational data of stellar abundances as well as progress in theoretical modeling of chemical evolution, significant discrepancies between theory and observation still remain for several elements. As one of such cases, it has been known that abundance behaviors of potassium (K) observed in old metal-poor stars do not well match theoretical predictions (see, e.g., Fig. 13 in Prantzos et al. 2018 and the references therein).

For the sake of ameliorating this situation, collecting reliable K abundances for as many stars as possible should be important. However, spectroscopically established abundance data published so far are not necessarily sufficient as long as this element is concerned. This is presumably due to the fact only the strong K I 7698.96 Å line of the doublet (hereinafter often referred to as "K I 7699") has to be invoked, since the paired line at 7664.90 Å (K I 7665) tends to be severely blended with telluric lines and

other potassium lines are generally too weak to be measurable. In addition, because of its conspicuous strength, special difficulties are involved with abundance determination from this line: one problem is the sensitivity to a choice of (often uncertain) damping parameters, but more important is that it suffers a considerable non-LTE effect.

Actually, pioneering studies of stellar K abundances done under the assumption of LTE (e.g., Gratton & Sneden 1987a,b; Chen et al. 2000) are not regarded as reliable as viewed from present-day standard. Meanwhile, efforts of investigating the non-LTE effect on K I 7699 by non-LTE calculations with sufficiently complex atomic model of K have been made by several investigators not only for the Sun (de la Reza & Müller 1975; Bruls et al. 1992; Zhang et al. 2006a) but also for stars of other types (Takeda et al. 1996; Ivanova & Shimanskiĭ 2000; Takeda et al. 2002; Shimansky et al. 2003; Zhang et al. 2006b; Andrievsky et al. 2010; Reggiani et al. 2019). Making use of these theoretical accomplishments, chemical evolution studies of potassium based on the non-LTE abundances derived from K I 7699 have gradually emerged

since the beginning of this century, where the targets of those investigations are roughly divided into two groups: (i) mildly metal-poor or metal-rich stars of disk population ($-1 \lesssim$ [Fe/H] $\lesssim 0.5$) (Takeda et al. 2002; Zhang et al. 2006b; Wang et al. 2009; Zhao et al. 2016; Reggiani et al. 2019) and (ii) very metal-poor stars of halo population($-4 \lesssim$ [Fe/H] $\lesssim -2$) (Cayrel et al. 2004; Takeda et al. 2009; Andrievsky et al. 2010; Roederer et al. 2014; Reggiani et al. 2019).

The focus of this study is placed on the former mildly metal-poor or metal-rich stars belonging to the galactic disk population. A problem regarding this group to be clarified is that the behaviors of [K/Fe][1] vs.[Fe/H] relation (an important diagram for investigating the nucleosynthesis evolution of K in the Galaxy) derived for disk stars by several previous studies are not necessarily consistent with each other in the quantitative sense. Takeda et al.'s (2002) non-LTE reanalysis on Chen et al.'s (2000) spectra of thin-disk stars resulted in a progressive increase of [K/Fe] with a decrease in [Fe/H] from [K/Fe] ~ -0.1 (at [Fe/H] ~ 0) to [K/Fe] $\sim +0.3$ (at [Fe/H] ~ -1) (cf. Fig. 4a therein), suggesting d[K/Fe]/d[Fe/H] ~ -0.4. Meanwhile, Zhang et al.'s (2006b; cf. Fig. 5 therein) results for thin-disk stars ($-0.8 \lesssim$ [Fe/H] $\lesssim -0.2$) as well as Wang et al.'s (2009; cf. Fig. 9c therein) analysis on thin-disk stars ($-0.5 \lesssim$ [Fe/H] $\lesssim +0.4$) showed a similar linear tendency but appreciably steeper gradient (d[K/Fe]/d[Fe/H] ~ -0.6). In contrast, Zhao et al.'s (2016) Fig. 9 suggests a shallower slope of d[K/Fe]/d[Fe/H] ~ -0.2 to -0.3 for thin-disk stars ($-0.8 \lesssim$ [Fe/H] $\lesssim +0.2$). Which of these represents the actual trend of disk stars at all?

Here, the following points may be worth consideration:
— First, the number of stars analyzed by each of these studies is only around ~ 20, which is not sufficient for elucidating statistically meaningful tendency. Considerably increasing the sample size (ca., up to the order of $\sim 10^2$) would undoubtedly improve the situation.
— Second, all these previous K abundance studies for disk-population stars made use of late F–early G dwarfs, but red giants (of disk metallicity)[2] seem to have never been employed for this purpose. Since potassium is not expected to suffer any change by evolution-induced dredge-up (unlike lighter elements such as CNO or Na), primordial K abundances should be retained at the surface of giants. Then, why not use red giants (which are intrinsically bright and available in large numbers) for investigating the chemical evolution of K in the disk of the Galaxy?
— Third, since [Fe/H] is roughly related to stellar age (i.e., older stars tend to have lower [Fe/H]), it is worthwhile to examine age-dependence of [K/Fe] if possible, since pro-

gressive increase with age may as well be detected if [K/Fe] grows with a lowering of [Fe/H]. In this context, it is interesting that recent Spina et al.'s (2016) high-precision differential abundance study on the solar twins of widely different ages showed that [K/Fe] is almost age-independent (unlike other elements which revealed systematic trend with age). The successsive non-LTE reanalysis of Spina et al.'s (2016) data by Reggiani et al. (2019) again resulted in almost the same conclusion. As such, this point should be worth reinvestigation based on a large number of stars with known ages.

Motivated by these notions, this study aims at determining the non-LTE K abundances from the K I 7699 line for an extensive sample of 160 late F–early K dwarfs as well as 328 late G–early K giants (239 nearby giants and 89 giants in the *Kepler* field) belonging to the disk population ($-1 \lesssim$ [Fe/H] $\lesssim 0.5$), for which the spectra are conveniently available to the author and the stellar parameters are already determined (especially, stellar ages are known for FGK dwarfs and *Kepler* giants). The points of interest to be checked upon are as follows:

- How are the [K/Fe] vs. [Fe/H] relations derived for each of the groups (dwarfs, nearby giants, and *Kepler* giants) compared with each other? Are they consistent, or any difference is seen?
- What about the slope (d[K/Fe]/d[Fe/H]) of the resulting [K/Fe] values in comparison with the diversified gradients reported by previous studies?
- Is any systematic trend observed in [K/Fe] with stellar age?

2. Observational Data and Stellar Parameters

All the observational materials and stellar parameters employed for this investigation are those already used and determined in the previous studies of the author's group.

2.1. FGK dwarfs

Regarding dwarfs (including subgiants), the spectra of 160 stars observed in 2000–2003 with the 1.9 m reflector (+HIDES spectrograph) at Okayama Astrophysical Observatory (OAO) and published by Takeda et al. (2005a) were used. Besides, the Moon spectrum (substitute for the reference solar spectrum) was also taken from this database. The atmospheric parameters [$T_{\rm eff}$ (effective temperature), $\log g$ (surface gravity), $v_{\rm t}$ (microturbulence), and [Fe/H] (Fe abundance relative to the Sun)] of these 160 stars were determined from the equivalent widths measured for a number of selected Fe I and Fe II lines, while requiring that abundances do not depend upon χ (lower excitation potential) as well as W (equivalent width) and that mean abundances derived from Fe I and Fe II lines are equal (cf. Takeda et al. 2005b). Regarding the atmospheric parameters of Sun, $T_{\rm eff,\odot} = 5780$ K, $\log g_{\odot} = 4.44$, $v_{\rm t,\odot} = 1.0$ km s^{-1}, and [Fe/H]$_{\odot} = 0.00$ were employed (note that practically the same values were empirically derived with this method using Fe I/Fe II lines applied the Moon spectrum; cf.

---

[1] As usual, [X/Y] is the logarithmic abundance ratio of element X to element Y relative to the Sun; i.e., [X/Y] $\equiv (A_{\rm star}^{\rm X} - A_{\odot}^{\rm X}) - (A_{\rm star}^{\rm Y} - A_{\odot}^{\rm Y})$, where $A^{\rm X}$ is the logarithmic number abundance of element X normalized with $A^{\rm H} = 12$ (the suffix $\odot$ denotes the solar value).

[2] In contrast, studies of K abundances in very metal-poor halo stars predominantly invoked evolved giants (e.g., Cayrel et al. 2004); thus the situation is markedly different from the case of galactic disk stars.

Takeda et al. 2005b). Takeda (2007) evaluated the age ($\log age$) and mass (M) for each of these 160 stars by comparing the position in the $\log L$ (L: bolometric luminosity) vs. $\log T_{\mathrm{eff}}$ diagram with theoretical stellar evolutionary tracks. These stellar parameters are summarized in tableE1.dat (online material).

2.2. Nearby giants

As to giants, the spectra of 239 late G or early K giants were used, which were observed in 2012–2013 with the 1.9 m telescope and HIDES spectrograph at OAO and described in Takeda et al. (2015). These 239 stars (apparently bright with $V < 6$ mag and comparatively near to us within several hundreds parsec) are the subset of 322 giants targeted by the Okayama Planet Search Program. for which the atmospheric parameters (T_{eff}, $\log g$, v_{t}, and [Fe/H]) were already established by Takeda et al. (2008) in the same way as done for 160 dwarfs mentioned above. However, the mass values (closely related to stellar age) of these giants estimated by Takeda et al. (2008) are likely to be appreciably overestimated and unreliable for a number of red clump stars (constituting the majority of these sample stars), because of the difficulty in discriminating the evolutionary status of each star by using such a coarse grid of theoretical stellar evolutionary tracks as applied in that paper (cf. Takeda & Tajitsu 2015; Takeda et al. 2016 for more details). Accordingly, mass and age are treated as undetermined and not mentioned in this paper for these 239 giants, for which only four atmospheric parameters are presented in tableE2.dat (online material).

2.3. Kepler giants

In addition, as another set of giant stars, the spectra of late G–early K giants in the *Kepler* field observed with the 8.2 m Subaru Telescope (+ HDS spectrograph) on 2014 September 9 (42 stars) and 2015 July 3 (47 stars)[3] were also employed. Their atmospheric parameters were already determined spectroscopically by Takeda & Tajitsu (2015) and Takeda et al. (2016) in same manner as the cases of dwarfs and nearby giants described above. The distinct merit of these *Kepler* field giants is that the stellar mass (M) as well as the evolutionary status of each star are confidently established by making use of the seismological information, by which the stellar age can be reliably determined with the help of stellar evolutionary tracks as done by Takeda et al. (2016). In tableE3.dat (online material) are given the values of T_{eff}, $\log g$, v_{t}, [Fe/H], M, and $\log age$ for these 89 giant stars.

2.4. Comparison between the groups

The mutual comparisons of T_{eff}, $\log g$, v_{t}, and [Fe/H] are depicted in Figures 1a–1d, in order to illustrate the dif-

ference or similarity of these star groups. The discussions regarding correlations between these parameters are presented in Takeda et al. (2005b) and Takeda et al. (2008) for the case of dwarfs and giants, respectively.

Figures 1e and 1f also show the positional distributions of the program stars in the XYZ-space, where $X \equiv d \cos b \cos l$, $Y \equiv d \cos b \sin l$, and $Z \equiv d \sin b$ (d: distance from the Sun, l: galactic longitude, and b: galactic latitude). It can be seen from these figures that, while 160 dwarfs (within several tens parsec) as well as 239 nearby giants (within several hundreds parsec) are solar neighborhood stars as viewed from the galactic scale, 89 *Kepler* giants widely distribute with diversified distances from $\sim 10^{2}$ pc up to ~ 2 kpc in the confined direction to Cygnus. Accordingly, from the viewpoint of location in the Galaxy. the former two groups (dwarfs, nearby giants) are almost similar but the last group (*Kepler* giants) is distinctly different.

3. Kinematic Properties

3.1. Space velocities and orbital parameters

Examining the kinematic properties of stars is important for understanding to which stellar population they belong. Takeda (2007) computed the orbital motions within the galactic gravitational potential for the 160 FGK stars (program stars of this study) by using the positional data and the velocity data (proper motions and radial velocity), and derived R_{m} (mean galactocentric distance), e (orbital eccentricity), z_{max} (maximum separation from the galactic plane). These orbital quantities along with the space velocity components relative to the Local Standard of Rest (U_{LSR}, V_{LSR}, W_{LSR}) are presented in electronic tableE2 (kinepara.dat) of that paper.

Likewise, Takeda et al. (2008) carried out similar analysis of kinematic properties for 322 red giants (from which 239 nearby giants for this study were selected), and the resulting parameters are given in electronic tableE1 (kinepara.dat) of that paper.

These kinematic parameters for 89 giants in the *Kepler* field were newly computed for this investigation, following the same way as done in Takeda (2007). Regarding the parallax and proper motion data, the *Gaia* DR2 database (Gaia Collaboration et al. 2016, 2018) was invoked, while the values measured from our Subaru HDS spectra were used for radial velocities (they were confirmed to be consistent with *Gaia* DR2 data). The resulting orbital parameters and space velocity components are given in tableE4.dat of the online material.

3.2. Classification of stellar population

According to Ibukiyama & Arimoto (2002), the z_{max} vs. V_{LSR} (rotation velocity component) diagram can be used for discriminating thin-disk, thick-disk, and halo populations, as already done by Takeda (2007) and Takeda et al. (2008) to examine the stellar populations of FGK dwarfs and nearby giants. Figure 2a (reproduction of Fig. 14d in Takeda 2007), Figure 2b (similar to Fig. 9a in Takeda et al. 2008), and Figure 2c illustrate this situation for

---

[3] Actually, 48 stars in the *Kepler* field were observed in this observing run. However, for the case of KIC 7341231 which is a very metal poor subgiant with especially large (negative) radial velocity ($V_{\mathrm{r}}^{\mathrm{hel}} \simeq -270$ km s^{-1}), the K I 7699 line unfortunately fell on the gap of the echelle format at 7687–7694 Å and could not be used. Therefore, this star had to be excluded from this study.

160 FGK dwarfs, 239 nearby giants, and 89 *Kepler* giants, respectively. From these figures, 6 (out of 160) dwarfs, 5 (out of 239) nearby giants, and 13 (out of 89) *Kepler* field giants were concluded to be of thick-disk population (indicated by open symbols in the figures; see ReadMe.txt in online material for their specific IDs), while all others are of thin-disk population.

3.3. Relation to metallicity and age

Figures 2d–2l also depict the correlations between the space velocity $|v_{LSR}|$ ($\equiv \sqrt{U_{LSR}^2 + V_{LSR}^2 + W_{LSR}^2}$), metallicity ([Fe/H]), and stellar age. It can be read from these figures that (1) thick-disk stars tend to be old, metal-poor, and moving faster as compared to thin-disk stars, (2) lower-metallicity stars as well as older stars are apt to have higher space velocity, and (3) there is a tendency of older stars having lower metallicity; all these trends are natural and reasonably understood.

4. Determination of K abundances

4.1. Spectrum-fitting analysis

Although most of the previous studies mentioned in Section 1 determined the potassium abundances from the equivalent widths (W) of K I 7699 line, precisely measuring W is not necessarily an easy task for such a strong line often showing appreciable damping wings. In this investigation was instead adopted a spectrum-fitting approach for establishing the non-LTE K abundances of the program stars.

The procedure is similar to the one adopted in Takeda et al. (1996), which accomplishes the best fit between theoretical and observed profiles by finding the most optimum solutions of three parameters [A(K) (K abundance)[4], v_M (macrobroadening parameter),[5] and $\Delta\lambda$ (wavelength shift)], while applying the numerical algorithm described in Takeda (1995).

That is, unbroadened non-LTE theoretical profile, which was calculated for the relevant model atmosphere and non-LTE departure coefficients (specified by T_{eff}, $\log g$, and [Fe/H]) along with the given microturbulence (v_t), was broadened (by convolving the broadening function corresponding to v_M) and shifted (by $\Delta\lambda$) in order to be compared with the observed profile. The model atmosphere of each star was generated by interpolating Kurucz's (1993) ATLAS9 model grid in terms of T_{eff}, $\log g$, and [Fe/H], as done in Takeda (2007) or Takeda et al. (2008). Similarly, the depth-dependent non-LTE departure coefficients of the relevant levels (i.e., ground level and first excited level) were derived by interpolating the extensive grid computed in Takeda et al. (2002; cf. Appendix therein). Regarding the atomic parameters of the K I 7699 line, the same values as used in Takeda et

al. (2002) were adopted (cf. Sect. 4 therein). Appendix shows that Takeda et al.'s (2002) non-LTE calculations, upon which ths study is based, are in reasonable agreement with the recent ones of Reggiani et al. (2019).

This method turned out successful and a satisfactory fit could be accomplished for almost all cases, as demonstrated in Figure 3 (160 FGK dwarfs + Moon), Figure 4 (239 nearby giants) and Figure 5 (89 *Kepler* giants). Note that, since telluric lines (or spectrum defects) sometimes invaded into the fitting range depending on the radial velocity, they had to be masked and neglected in judging the goodness of fitting (as highlighted in green in these figures).

4.2. Equivalent widths and non-LTE corrections

Although the non-LTE K abundance (A) of each star could be established based on the spectrum-fitting technique as such, only this information would not suffice. In order for understanding the behaviors of resulting abundances (e.g., sensitivity to stellar parameters) differing from star to star, abundance-related quantities such as equivalent width (W) or non-LTE correction (Δ) are quite useful. Therefore, by using Kurucz's (1993) WIDTH9 program which was considerably modified by the author (e.g., to enable inclusion of non-LTE effect). the corresponding W of K I 7699 was evaluated by using the solution of A along with the same model atmosphere and v_t. Furthermore, based on such calculated W, the non-LTE abundance (A^{NLTE}) and LTE abundance (A^{LTE}) were inversely derived, from which the non-LTE abundance correction (Δ) was obtained as $A^{NLTE} - A^{LTE}$. The resulting W, A^{NLTE}, and Δ values are presented in tableE1.dat (FGK dwarfs), tableE2.dat (nearby giants), and tableE3.dat (*Kepler* giants) of the online material.

Figure 6 illustrates how W and Δ depend on T_{eff} and $\log g$ and how they correlate with each other. Roughly speaking, $W/|\Delta|$ tends to decrease/increase with higher T_{eff} or lower $\log g$ (cf. Figures 6a–6d), as long as stars belonging to the same group (e.g., 'dwarfs' group or 'giants' group) are concerned. According to Figure 6e, the extent of Δ tends to diminish as W increases. This is due to the fact that comparatively weaker lines (100 mÅ $\lesssim$ $W \lesssim$ 200 mÅ) are most saturated (i.e., line-forming layer is high) at the shoulder or the flat part of curve of growth and suffer an especially large non-LTE effect, while those stronger lines (200 mÅ $\lesssim W \lesssim$ 300 mÅ) are already in the damping part and comparatively less sensitive to a non-LTE effect (because deep-forming damping wings appreciably contribute to the total strength of such a strong line). This situation is elucidated in Figure 6f, where $\log W$ is plotted against $A^{NLTE} + (\chi_{ion} - \chi_{exc})5040/T_{eff}$ (χ_{ion} = 4.34 eV, χ_{exc} = 0.00 eV), which may be regarded as the abscissa of curve of growth (controlling the A- and T_{eff}-dependence of line strength).

---

[4] As usual, A(X) is the logarithmic number abundance of element X normalized as A(H) = 12: i.e., A(X) = $\log[N(X)/N(H)] + 12$.

[5] This v_M is the e-folding half width of the Gaussian macrobroadening function $f_M(v) \propto \exp[-(v/v_M)^2]$, which is regarded as a combination of (i) instrumental broadening, (ii) macroturbulence broadening, and (iii) rotational broadening.

5.   Behaviors of Potassium Abundances

5.1.   [K/Fe] vs. [Fe/H] relation

The [K/Fe] ratios of the program stars were calculated from the potassium abundances determined in Section 4 as

$$[K/Fe] \equiv (A^{\mathrm{NLTE}} - A_{\odot}^{\mathrm{NLTE}}) - [Fe/H], \tag{1}$$

where $A_{\odot}^{\mathrm{NLTE}}$ is the solar potassium abundance of 4.96 derived from the spectrum of Moon.

Takeda et al. (2002) discussed the ambiguities involved with the potassium abundances they derived from K I 7699 caused by uncertainties in atmospheric parameters (see Sect. 5 therein). In this investigation, the adopted values of T_{eff}, $\log g$, v_{t}, and [Fe/H] of all program stars are those consistently determined by the same method using Fe lines, and their statistical errors are typically several tens of K, $\lesssim 0.1$ dex, ~ 0.1 km s^{-1}, and a few hundredths of dex, respectively (cf. Takeda et al. 2005b, 2008). By combining these uncertainties with the results of Takeda et al. (2002), the typical errors in [K/Fe] may be estimated as $\lesssim 0.1$ dex.

The resulting [K/Fe] vs. [Fe/H] diagrams for each of the three stellar groups are displayed in Figures 7a–7c, where the corresponding non-LTE corrections are also shown. The characteristic trends recognized from these figures are summarized below:

- Generally, a qualitative trend is seen that [K/Fe] tends to increases with a decrease in [Fe/H], which is commonly seen in each of the groups (though specific details are different).
- Almost all thick-disk stars (indicated by open symbols in the figures) have supersolar [K/Fe] (> 0), mainly because they tend to be appreciably metal-poor ([Fe/H] < 0).
- Regarding the group of dwarf stars, [K/Fe] vs. [Fe/H] relation shows a tight tendency with small dispersion (cf. Figure 7a). Only one exceptional outlier is HD 50554, which exhibits a very large [K/Fe] of $+0.74$ despite its near-solar metallicity ([Fe/H] $= -0.03$); but the reason for this anomaly is unclear.
- Nearby giants reveal a rather similar trend to the case of dwarfs, though the dispersion is apparently larger and the slope appears to be slightly steeper, while several outliers with appreciably large [K/Fe] (> 0) exist even around the solar metallicity (cf. Figure 7b).
- However, a different feature is recognized for the case of giants in the *Kepler* field (cf. Figure 7c). Here, while the increasing trend of [K/Fe] towards lowered metallicity is still roughly seen by the existence of thick-disk stars, [K/Fe] values are generally enhanced (i.e., tending to be supersolar irrespective of the metallicity) with a considerable scatter. This implies that the chemical evolution history of these *Kepler* giants would have been dissimilar to that of solar neighborhood stars. The reason why they show

so diversified [K/Fe] may be due to their widely scattered locations along the direction to Cygnus (cf. Figures 1e and 1f).

5.2.   Comparison between dwarfs and giants

It is not easy to evaluate the quantitative characteristics of [K/Fe] (e.g., gradient with respect to a change in [Fe/H]) in Figures 7a–7c only by eye-inspection, because the plotted points are densely overlapped. Therefore, mean $\langle [K/Fe] \rangle$ (and the corresponding standard deviation) were computed by averaging the [K/Fe] values[6] included at each of the seven metallicity bins ($\Delta[Fe/H] = 0.1$dex at $-0.5 \leq [Fe/H] \leq +0.2$) for three star groups, and comparisons were made for nearby giants vs. FGK stars as well as *Kepler giants* vs. FGK dwarfs, as shown in Figures 8a and 8b. The linear-regression analysis applied to these $\langle [K/Fe] \rangle$ data yielded the following relations: $\langle [K/Fe] \rangle = -0.129(\pm 0.022) \times [Fe/H] - 0.008(\pm 0.005)$ (FGK dwarfs), $\langle [K/Fe] \rangle = -0.157(\pm 0.013) \times [Fe/H] + 0.004(\pm 0.003)$ (nearby giants), and $\langle [K/Fe] \rangle = -0.100(\pm 0.063) \times [Fe/H] + 0.049(\pm 0.016)$ (*Kepler* giants), where the values in parentheses (denoted in Italics) are the standard errors. These lines are also drawn in the figures.

Figure 8a suggests that the [K/Fe] trend of nearby giants is not much different from that of FGK dwarfs (though marginally higher [K/Fe] by a few hundredths dex and slightly steeper slope), while *Kepler* giants and dwarfs (shown in Figure 8b) are in disagreement with each other as already mentioned (the former show systematically larger [K/Fe] values at the same metallicity). Consequently, it can be concluded that (1) nearly consistent [K/Fe] vs. [Fe/H] relations could be derived from this investigation for both dwarfs and giants as long as stars in the solar neighborhood are concerned, (2) but the giants in the *Kepler* field are different presumably because they are in diversified locations far from the Sun where chemical evolution history would have been more or less variant.

According to Figure 8a, the d[K/Fe]/d[Fe/H] gradient corresponding to galactic disk dwarfs in the solar neighborhood (within several tens parsecs) is concluded to be ~ -0.1 to -0.15, while that for nearby giants (within several hundreds parsec) is similar around ~ -0.15. Regarding the questions raised in Section 1 (i.e., which of the variously reported slopes are correct), the resulting d[K/Fe]/d[Fe/H] gradient for thin-disk population derived from this investigation (from ~ -0.1 to -0.15) is shallower than any of the past studies, though the recent Zhao et al.'s (2016) consequence (~ -0.2 to -0.3) is reasonably the closest among these. That these previous authors obtained diversified results of comparatively steeper slope (from ~ -0.2 to -0.6) may have originated from the paucity of their sample stars.

---

[6]   In the averaging process, the data showing appreciable deviations within each bin-group were discarded, which were judged by Chauvenet's criterion (Taylor 1997).

5.3. Relation to stellar ages

Finally, how the resulting [K/Fe] depends on the stellar age is examined, which is possible for FGK dwarfs and *Kepler* giants (ages are not available for nearby giants; cf. Section 2.2). An inspection of Figure 7d reveals that a systematic but subtle increase exists in [K/Fe] with age for these dwarfs in the solar neighborhood, which means that [K/Fe] in the gas of the solar neighborhood gradually evolved from $\sim +0.1$ ($\sim 10^{10}$ yr ago) to [K/Fe] ~ 0 ($\sim 5 \times 10^9$ yr ago when the Sun was born) and further down to ~ -0.1 ($\sim 10^9$ yr ago). In contrast, any clear age-dependence is hardly observed in the [K/Fe] values of *Kepler* giants (cf. Figure 7f), which is presumably because stars having experienced diversified chemical enrichment histories are mixed up in this sample.

As mentioned in Section 1, precisely determined [K/Fe] values for solar analog stars (with various stellar ages from $\sim 10^9$ yr to $\sim 10^{10}$ yr) determined by Spina et al. (2016) and Reggiani et al. (2019) (non-LTE reanalysis) did not show any clear dependence upon age, although most of their sample stars are in the solar neighborhood. It should be noted, however, that all those solar twins have almost the same metallicity as that of the Sun ([Fe/H] $\simeq 0$), despite that they have diversified ages (i.e., metallicity is not dependent upon age at all). Accordingly, since the target stars used in these two recent studies are rather specific, their results can not be directly compared with that of the present investigation based on a large number of nearby dwarfs showing a rough age–metallicity relation (cf. Figure 2j). As a possibility, it may be that the enrichment of K in the Galaxy significantly depends upon the local condition (i.e., not necessarily a unique function of time) and that [K/Fe] is more tightly bound to [Fe/H] rather than age; this might explain the reason why they could not detect any age-dependence in their sample solar analogs of [Fe/H] $\simeq 0$.

6.   Summary and Conclusion

Our understanding on the galactic chemical evolution of potassium is still insufficient, because the observed [K/Fe] relation can not be well reproduced by theoretical predictions. On the observational side, an embarrassing problem regarding galactic disk stars ($-1 \lesssim$ [Fe/H] $\lesssim +0.5$) is that the slopes of [K/Fe] vs. [Fe/H] relations derived by several previous studies are diversified and not consistent with each other, though the qualitative tendency (increasing [K/Fe] with a decrease in [Fe/H]) is the same. Besides, recent precision abundance analysis on solar twins of widely different ages reported that [K/Fe] is nearly constant around ~ 0 without showing any systematic trend with stellar age, which is hard to understand in context of expected evolution of [K/Fe] with time.

With an aim to shed light to clarifying these issues, an extensive determination of potassium abundances was carried out based on the non-LTE profile-fitting analysis of the K I 7699 line applied to a large sample of 488 stars (160 late F–early K dwarfs, 239 late G–early K nearby giants, and 89 late G–early K giants in the *Kepler* field), all belonging to the disk population ($-1 \lesssim$ [Fe/H] $\lesssim 0.5$), for which the spectra are available and the stellar parameters are already determined (stellar ages are known for FGK dwarfs and *Kepler* giants).

The main point of interest was to elucidate the observed behaviors of [K/Fe] in the galactic disk, where special attention was paid to (i) checking whether these different star groups (especially dwarfs vs. giants) yield consistent results with each other, (ii) clarifying the d[K/Fe]/d[Fe/H] gradient to compare with previous studies. and (iii) checking whether [K/Fe] shows any systematic trend with stellar age.

The qualitative trend turned out to be almost the same irrespective of the star group that [K/Fe] tends to increases with a decrease in [Fe/H]; especially, thick-disk stars of comparatively lower metallicity tend to have supersolar [K/Fe] (> 0). However, quantitative features are more or less different from group to group.

The [K/Fe] vs. [Fe/H] relation of dwarf stars shows a tight tendency with small dispersion, and nearby giants also exhibit an almost similar trend to the case of dwarfs, though the dispersion is somewhat larger with a slightly steeper slope and a marginal offset by a few hundredths dex. The corresponding mean d[K/Fe]/d[Fe/H] gradient for these two groups turned out rather shallow (~ -0.1 to -0.15 for dwarfs and around ~ -0.15 for giants). It may be concluded from these results that modestly consistent [K/Fe] trends with metallicity were obtained for both dwarfs and giants as long as those solar neighborhood stars are concerned.

As to the comparison with diversified [K/Fe] vs. [Fe/H] trends reported so far, the d[K/Fe]/d[Fe/H] gradient (~ -0.1 to -0.15) resulting from this investigation turned out to be shallower than any of the previous studies.

The [K/Fe] values of *Kepler* giants are generally enhanced by $\lesssim 0.1$ dex (tending to be supersolar irrespective of the metallicity) with a considerable scatter (making the gradient of [K/Fe] with respect to [Fe/H] rather ambiguous). This implies that the chemical evolution history of these *Kepler* giants would have been different from that of solar neighborhood stars. The reason why they show so diversified [K/Fe] may be due to their widely scattered locations.

Regarding the age-dependence of potassium abundance, a marginal trend of increasing [K/Fe] with stellar age is recognized for dwarfs, while any systematic tendency is not observed for *Kepler* giants. The reason why Spina et al. (2016) and Reggiani et al. (2019) could not detect any dependence upon age in the [K/Fe] values of nearby solar twins may be due to their specific samples (same metallicity stars of widely different ages). It may be possible that the galactic chemical evolution of K is not necessarily a monotonic function of time but more significantly depends upon the local condition, by which [K/Fe] would be more tightly bound to [Fe/H] rather than age.

Astronomical Observatory of Japan.

Appendix. Comparison with Reggiani et et.'s (2019) Non-LTE Calculations

Takeda et al. (2002; cf. Appendix therein) published the non-LTE equivalent widths and non-LTE corrections for both the K I 7699 and 7665 lines calculated on an extensive grid of 300 models resulting from combinations of five T_{eff} (4500, 5000, 5500, 6000, 6500), five $\log g$ (1.0, 2.0, 3.0, 4.0, 5.0), four [Fe/H] (0, -1, -2, -3), and three v_t (1, 2, 3) values. The adopted atomic data for the calculations were the same as used in Takeda et al. (1996). For example, regarding collisions with neutral hydrogen atoms (generally important in non-LTE calculations for late-type stars), the rates computed by the conventionally used classical formula were drastically reduced by multiplying by an empirically determined factor of $k(= 10^h) = 10^{-3}$; and as to van der Waals damping width (which plays a significant role in calculating profiles or equivalent widths of strong lines), the classically evaluated damping constant C_6^{classic} (so-called Unsöld approximation) was increased by an empirically established correction of $\Delta \log C_6 = +1.0$ (corresponding to multiplying the classical van der waals damping width $\Gamma_6^{\mathrm{classic}}$ by a factor of 2.5); see Takeda et al. (1996) for more details.

Very recently, Reggiani et al. (2019) conducted new non-LTE calculations for neutral potassium by using the realistic atomic data achieved by modern physics without invoking any classical formula or empirical corrections. They also published non-LTE equivalent widths and non-LTE corrections of K I 7699 and 7665 lines computed for a large number of models in the parameter range of 4000 K $\leq T_{\mathrm{eff}} \leq$ 8000 K, $0.5 \leq \log g \leq 5.0$, $-5.0 \leq$ [Fe/H] $\leq +0.5$, and three v_t of 1, 2, and 5 km s^{-1}.

It is interesting to check how Takeda et al.'s (2002) grids of non-LTE line strengths and abundance corrections are compared with those Reggiani et al.'s (2019) new calculations. Regarding the input K abundance, Takeda et al. (2002) adopted [K/Fe] $= -0.3, 0.0, +0.3$ for [Fe/H] $= 0$ models, while $+0.2, +0.5, +0.8$ for metal-poor [Fe/H] (< 0) models. In contrast, Reggiani et al. (2019) varied the K abundance 11 times as [K/Fe] $= -1.25, -1.00, -0.75, \cdots,$ $+1.00$, and $+1.25$) irrespective of [Fe/H]. Therefore, in order to enable a direct comparison at the same set of input parameters, comparisons are made only on the cases of K I 7699 line with [Fe/H] $=$ [K/Fe] $= 0$, $v_t = 2$ km s^{-1}, and combinations of ($T_{\mathrm{eff}} = 4500, 5000, 5500, 6000, 6500$) and ($\log g = 2, 3, 4, 5$).

The mutual comparisons of the non-LTE equivalent widths and non-LTE corrections are depicted in Figures 9a and 9b, respectively. We can see from these figures that both are in reasonable consistency, though W^{NLTE} (Reggiani) tends to be somewhat lower than W^{NLTE} (Takeda) when the line is very strong ($W \gtrsim 500$ mÅ) and Δ^{NLTE} (Reggiani) begins to deviate from Δ^{NLTE} (Takeda) near to $\Delta^{\mathrm{NLTE}} \sim -1$ (around the largest $|\Delta^{\mathrm{NLTE}}|$). Accordingly, it can be stated that Takeda et al.'s (2002) results based on their somewhat outdated calculations (upon which this study is based) are not significantly different from those of Reggiani et al.'s (2019) new non-LTE calculations using up-to-date atomic data.

References

Andrievsky, S. M., Spite, M., Korotin, S. A., Spite, F., Bonifacio, P., Cayrel, R., Françis, P., Hill, V. 2010, A&A, 509, A88

Bruls, J. H. M. J., Rutten, R. J., Schchukina, N. G. 1992, A&A, 265, 237

Cayrel, R., et al. 2004, A&A, 416, 1117

Chen, Y.-Q., Nissen, P. E., Zhao, G., Zhang, H. W., Benoni, T. 2000, A&AS, 141, 491

de la Reza, R., Müller, E. 1975, Sol. Phys., 43, 15

Gaia Collaboration et al. 2016, A&A, 595, A1

Gaia Collaboration et al. 2018, A&A, 616, A1

Gratton, R. G., Sneden, C. 1987a, A&A, 178, 179

Gratton, R. G., Sneden, C. 1987b, A&AS, 68, 193

Ibukiyama, A., Arimoto, N. 2002, A&A, 394, 927

Ivanova, D. V., Shimanskiǐ, V. V. 2000, Astron. Rep, 44, 376

Kurucz, R. L. 1993, Kurucz CD-ROM, No. 13 (Harvard-Smithsonian Center for Astrophysics)

Prantzos, N., Abia, C., Limongi, M., Chieffi, A., Cristallo, S. 2018, MNRAS, 476, 3432

Reggiani, H., et al. 2019, A&A, 627, A177

Roederer, I. U., Preston, G. W., Thompson, I. B., Shectman, S. A., Sneden, C., Burley, G. S., Kelson, D. D. 2014, AJ, 147, 136

Shimansky, V. V., Bikmaev, I. F., Galeev, A. I., Shimanskaya, N. N., Ivanova, D. V., Sakhibullin, N. A., Musaev, F. A., Galazutdinov, G. A. 2003, Astron. Rep., 47, 750

Spina, L., Meléndez, J., Karakas, A. I., Ramírez, I., Monroe, T. R., Asplund, M., Yong, D. 2016, A&A, 593, A125

Takeda, Y. 1995, PASJ, 47, 287

Takeda, Y. 2007, PASJ, 59, 335

Takeda, Y., et al. 2005a, PASJ, 57, 13

Takeda, Y., Kaneko, H., Matsumoto, N., Oshino, S., Ito, H., Shibuya, T. 2009, PASJ, 61, 563

Takeda, Y., Kato, K., Watanabe, Y., Sadakane, K. 1996, PASJ, 48, 511

Takeda, Y., Ohkubo, M., Sato, B., Kambe, E., Sadakane, K. 2005b, PASJ, 57, 27 [Erratum: PASJ, 57, 415]

Takeda, Y., Sato, B., Murata, D. 2008, PASJ, 60, 781

Takeda, Y., Sato, B., Omiya, M., Harakawa, H. 2015, PASJ, 67, 24

Takeda, Y., Tajitsu, A. 2015, MNRAS, 450, 397

Takeda, Y., Tajitsu, A., Sato, B., Liu, Y.-J., Chen, Y.-Q., Zhao, G. 2016, MNRAS, 457, 4454

Takeda, Y., Zhao, G., Chen, Y.-Q., Qiu, H.-M., Takada-Hidai, M. 2002, PASJ, 54, 275

Taylor, J. R. 1997, An Introduction to Error Analysis, The Study of Uncertainties in Physical Measurements, 2nd ed. (Herndon, V.A.: University Science Books)

Wang, X. M., Shi, J. R., Zhao, G. 2009, MNRAS, 399, 1264

Zhang, H. W., Butler, K., Gehren, T., Shi, J. R., Zhao, G.
  2006a, A&A, 453, 723
Zhang, H. W., Gehren, T., Butler, K., Shi, J. R., Zhao, G.
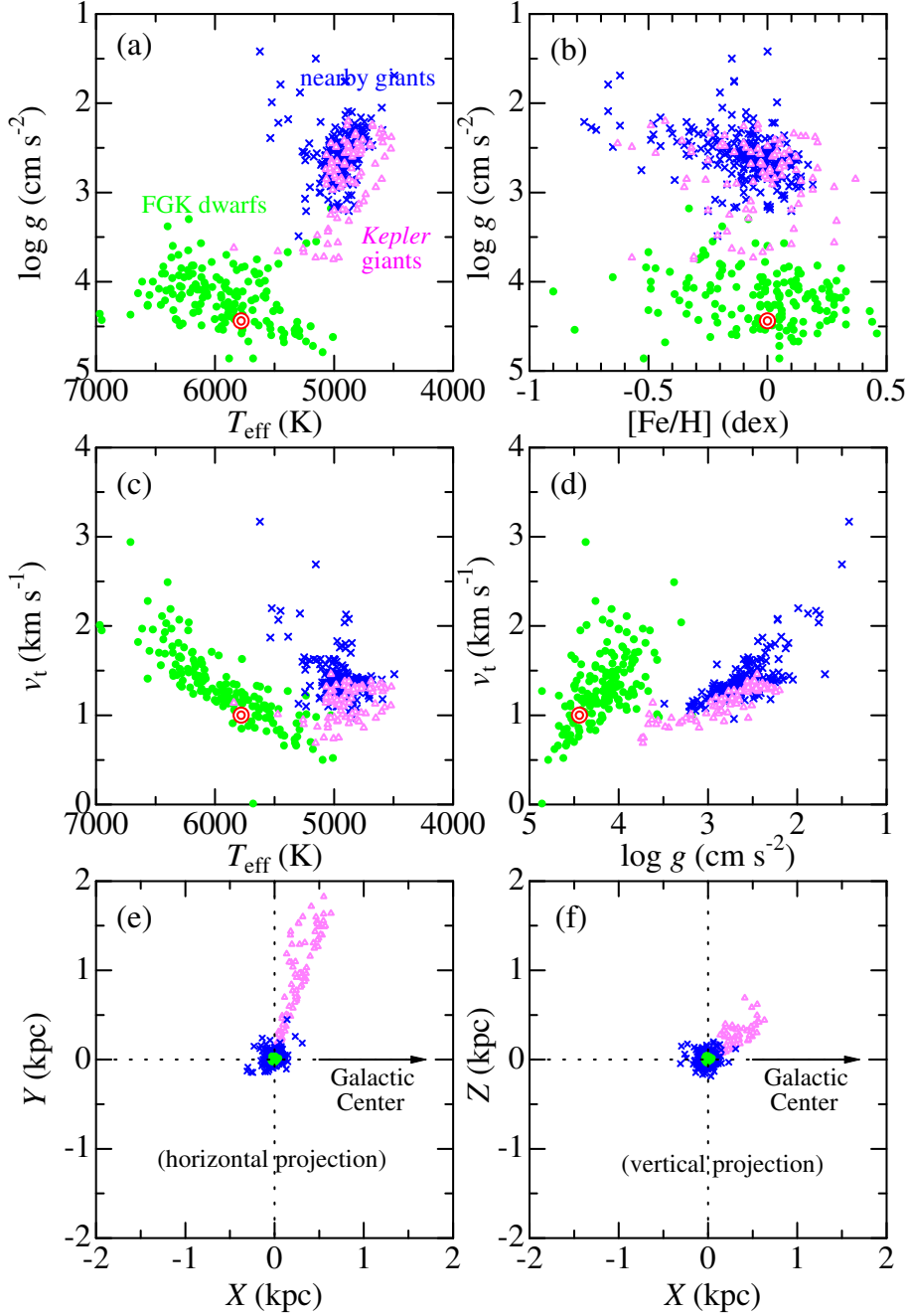 2006b, A&A, 457, 645
Zhao, G., et al. 2016, ApJ, 833, 225

Fig. 1. Panels (a)–(d) show the mutual correlations of adopted atmospheric parameters: (a) $\log g$ vs. T_{eff}, (b) $\log g$ vs. [Fe/H], (c) v_t vs. T_{eff}, and (d) v_t vs. $\log g$. The lower two panels (e) and (d) are the cross sectional diagrams projected onto the $Z = 0$ plane (galactic plane passing the Sun) and the $Y = 0$ plane (plane perpendicular to the galactic plane, passing the Sun and the galactic center), respectively, which illustrate the locations of the program stars in the Galaxy (Sun at the origin of $X = Y = Z = 0$). Three groups of program stars are distinguished by different symbols: green circles — 160 FGK dwarfs, blue crosses — 239 nearby giants, and pink triangles — 89 *Kepler* giants. The Sun is indicated by the red double circle.
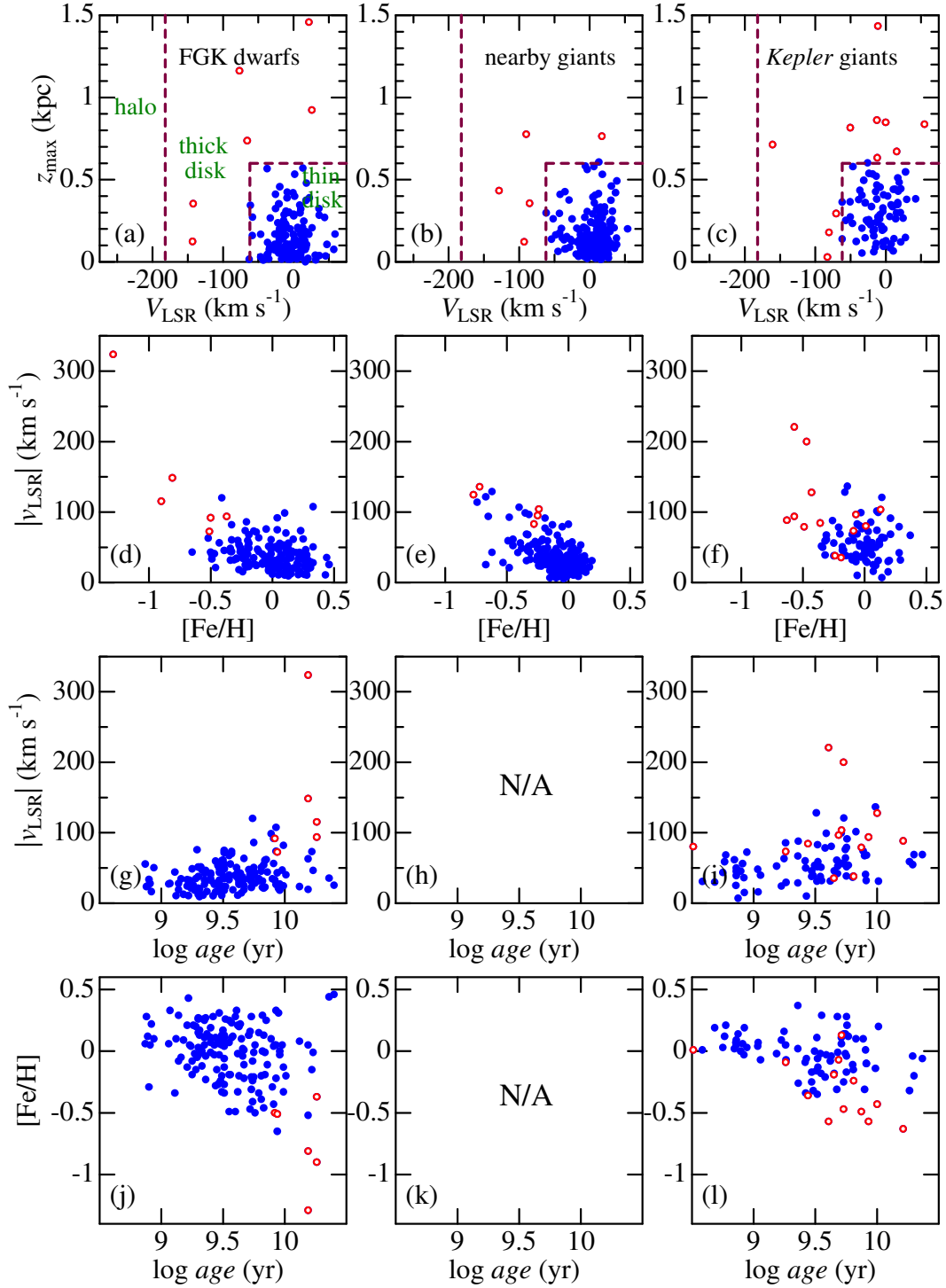
Fig. 2. In the top (1st) row are shown the correlation diagrams between the maximum separation from the galactic plane (z_{max}) and the rotation velocity component relative to LSR (V_{LSR}), which may be used for classifying the stellar population (the boundaries are indicated by the dashed lines; cf. Ibukiyama & Arimoto 2002). The extents of space velocities relative to LSR [$|v_{LSR}| \equiv (U_{LSR}^2 + V_{LSR}^2 + W_{LSR}^2)^{1/2}$] are plotted against [Fe/H] and *age* in the 2nd and 3rd rows, respectively. The *age* vs. metallicity ([Fe/H]) relations are depicted in the bottom (4th) panels. The left, middle, and right panels correspond to FGK dwarfs, nearby giants, and *Kepler* giants, respectively. Stars of thin-disk and thick-disk populations are indicated by (blue) filled and (red) open symbols, respectively. Note that, in panel (c), one star (KIC 2714397) of thick-disk population ($V_{LSR} = -181$ km s^{-1}, $z_{max} = 3.17$ kpc) is outside of the plot range.
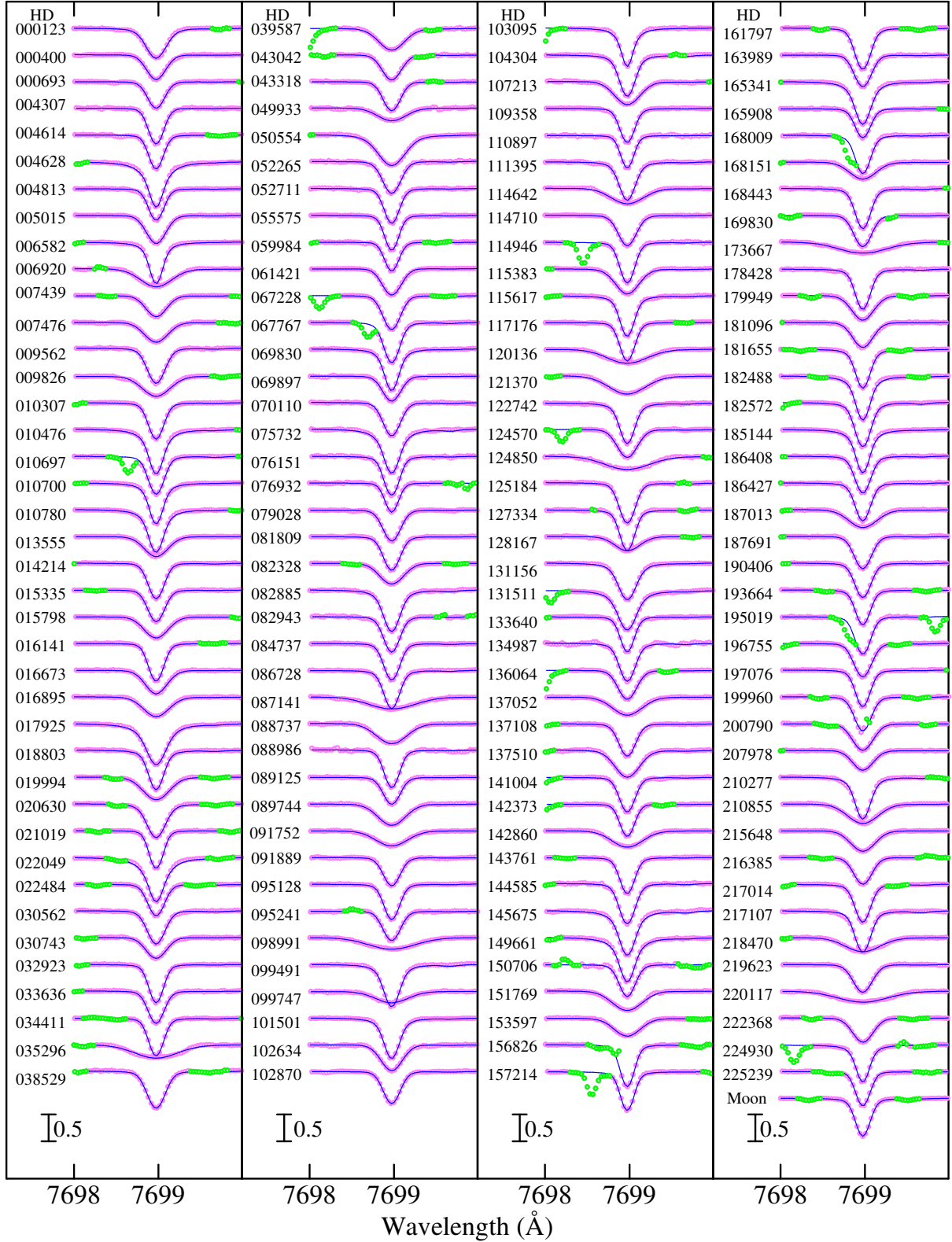
Fig. 3. Synthetic spectrum fitting for 160 FGK dwarfs/subgiants (and the Sun/Moon) in the region comprising the K I 7699 line. The best-fit theoretical spectra are shown by blue solid lines, and the observed data are plotted by pink open circles (while those masked/disregarded in the fitting are highlighted in green). A vertical offset of 0.5 (in terms of the normalized flux with respect to the continuum) is applied to each spectrum relative to the adjacent ones. Each of the spectra are arranged in the increasing order of star number (indicated on the left to each spectrum). The wavelength scale of each spectrum is adjusted to the laboratory frame.
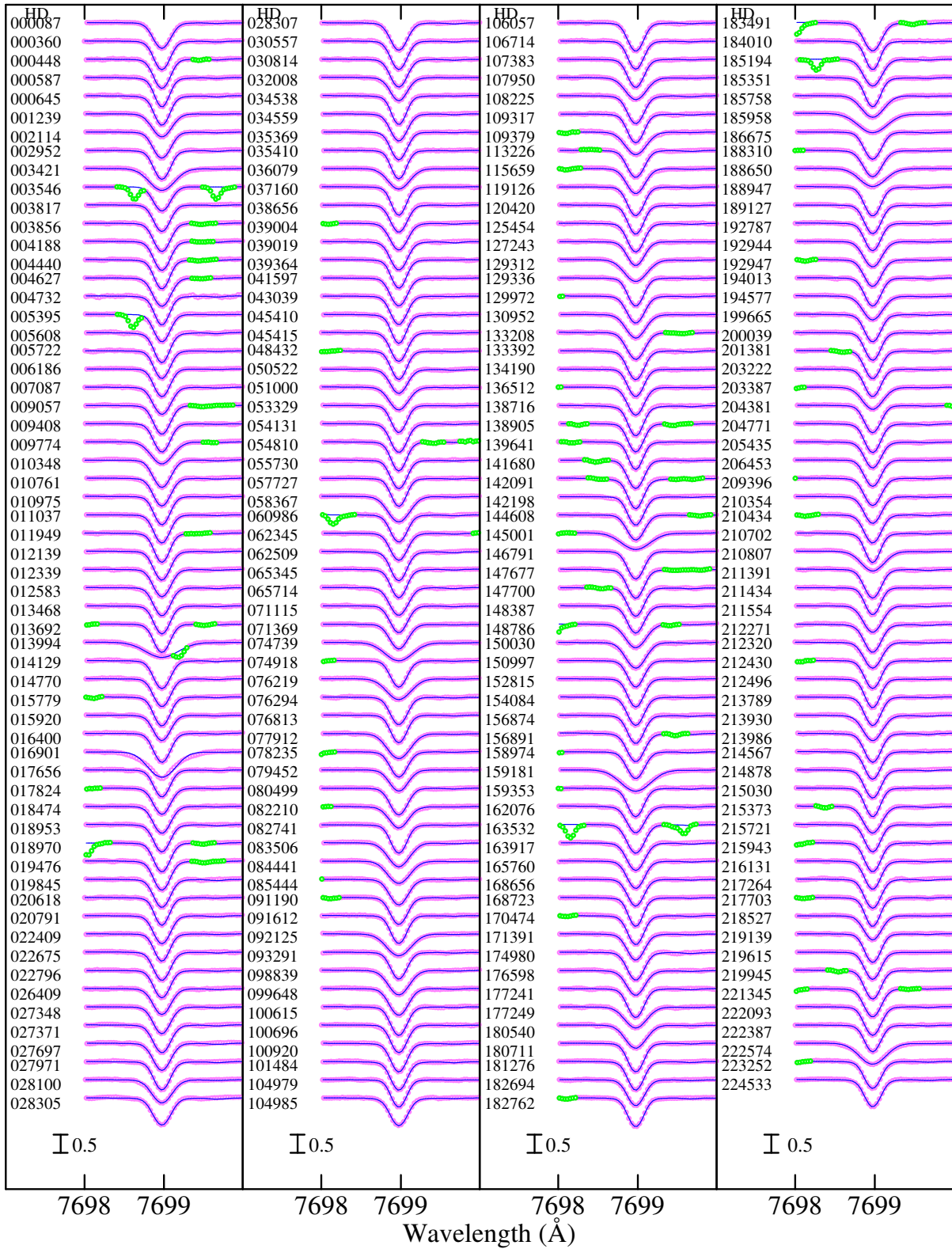
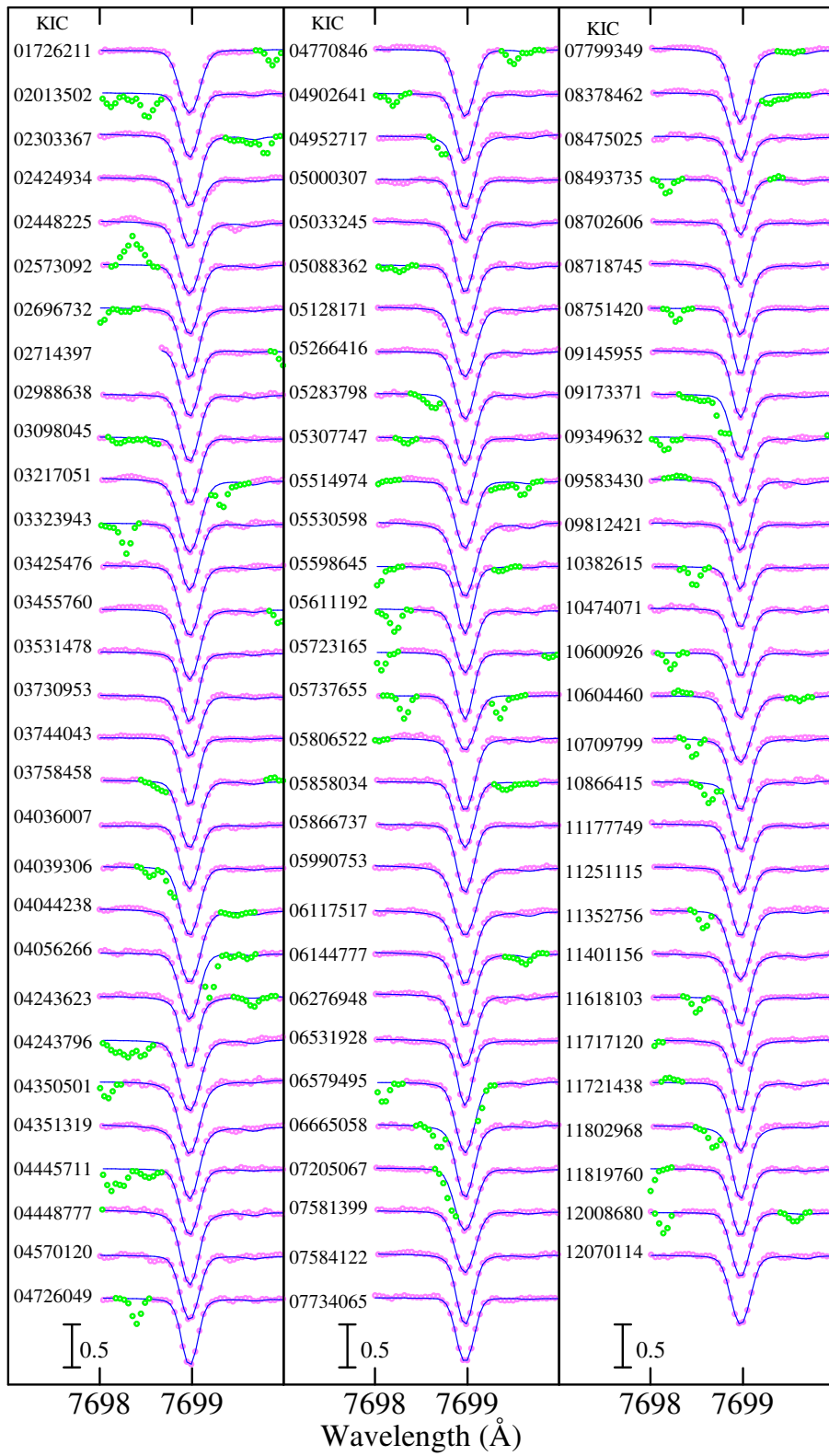**Fig. 4.** Synthetic spectrum fitting for 239 nearby red giants. Otherwise, the same as in Figure 3.

Fig. 5. Synthetic spectrum fitting for 89 giants in the *Kepler* field. Otherwise, the same as in Figure 3.
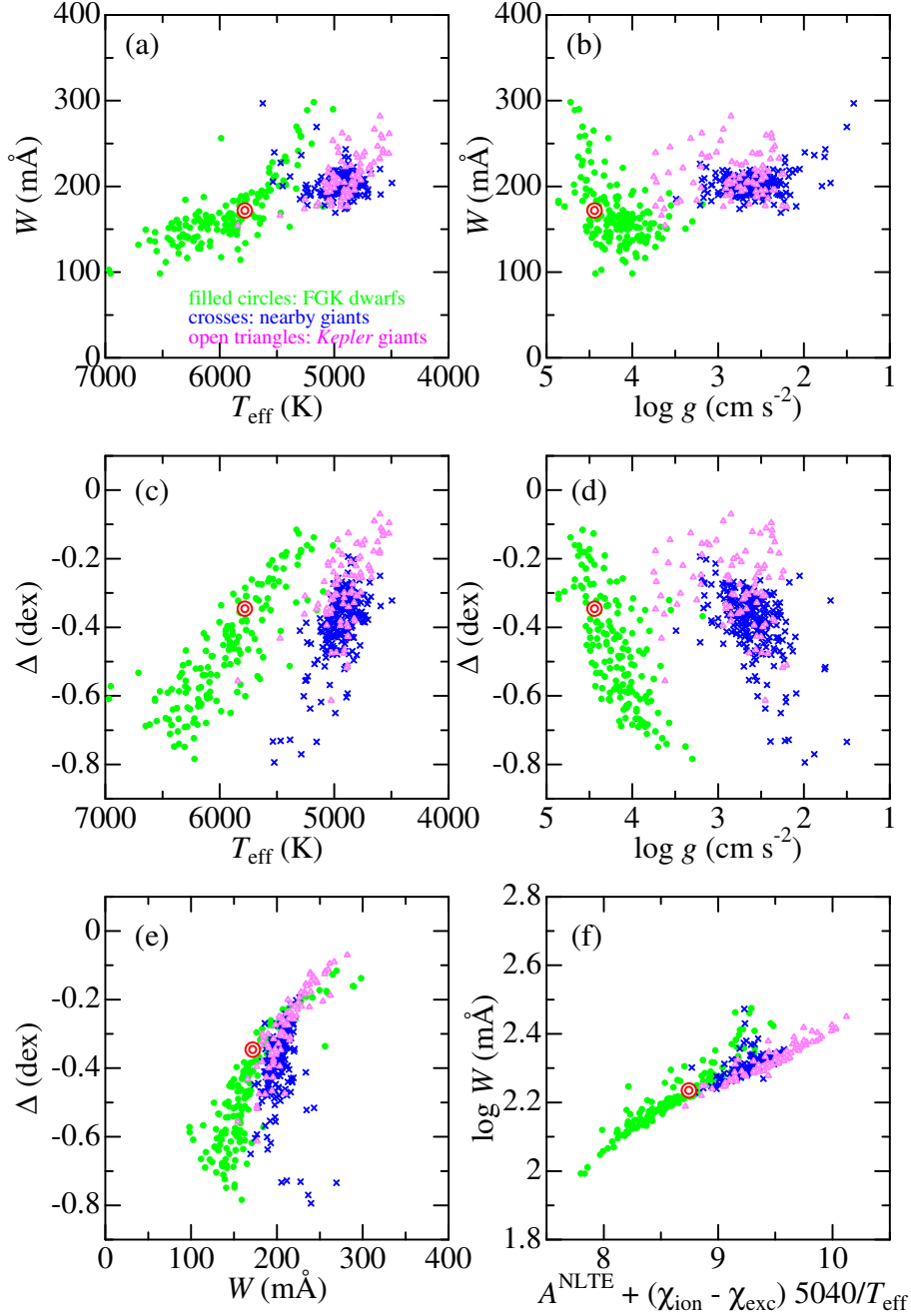
Fig. 6. Equivalent widths (W) of the K I 7699 line are plotted against $T_{\rm eff}$ and $\log g$ in panels (a) and (b), while the dependences of non-LTE corrections (Δ) upon $T_{\rm eff}$, $\log g$, and W are shown in panels (c), (d), and (e), respectively. In panel (f) are plotted the $\log W$ values against $A^{\rm NLTE} + (\chi_{\rm ion} - \chi_{\rm exc})5040/T_{\rm eff}$ (abscissa of curve of growth), where $A^{\rm NLTE}$ is the non-LTE abundance derived for each star and $\chi_{\rm ion}/\chi_{\rm exc}$ is the ionization/excitation potential (in eV). The same meanings of the symbols as in Figure 1.
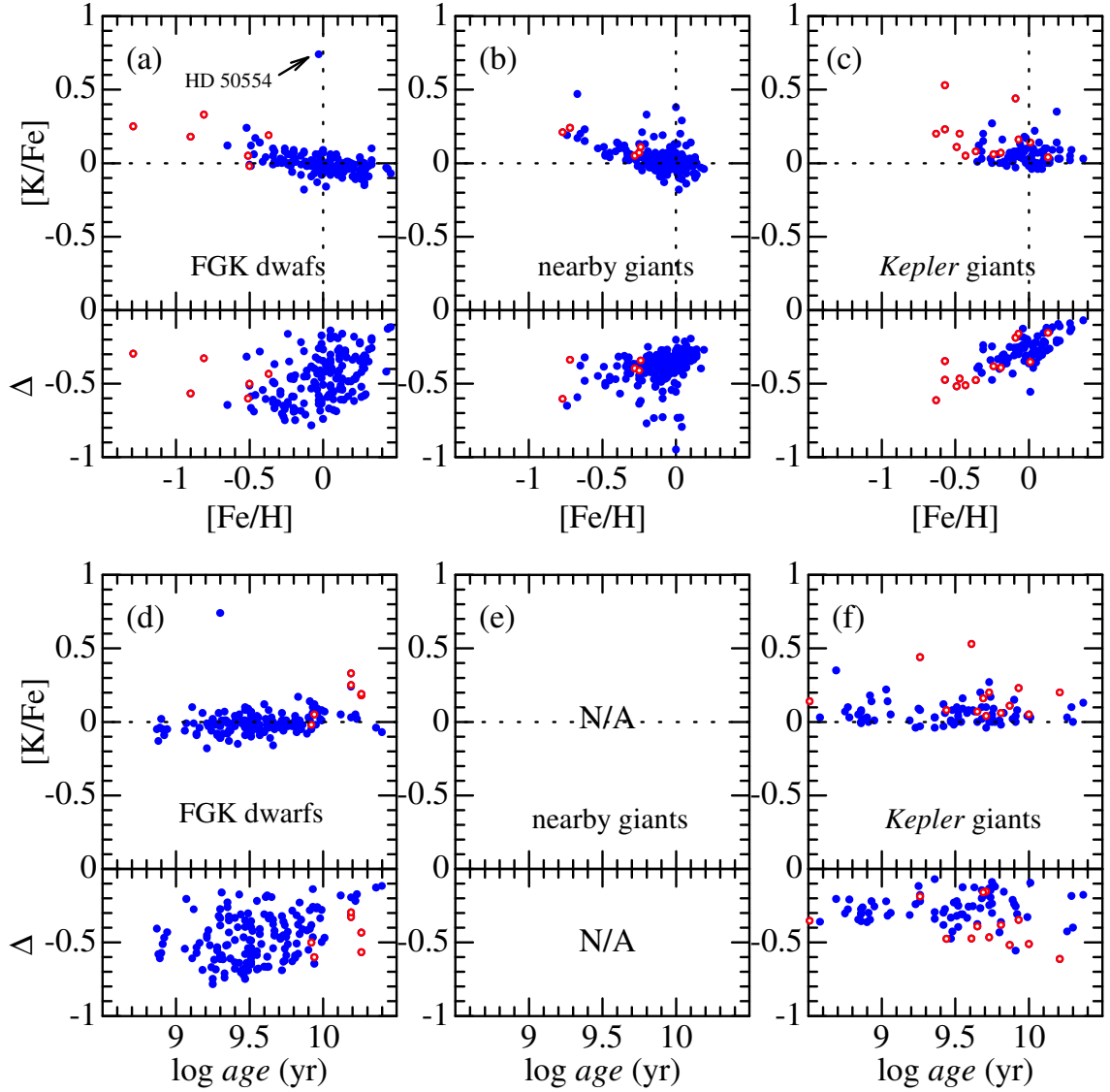
Fig. 7. The values of [K/Fe] (non-LTE K-to-Fe abundance ratio) and Δ (non-LTE correction) derived for each star are plotted against [Fe/H] (upper panels) and log *age* (lower panels), respectively. As in Figure 2, the left, middle, and right panels correspond to FGK dwarfs, nearby giants, and *Kepler* giants, respectively. Likewise, the same meanings of the symbols hold as in Figure 2.
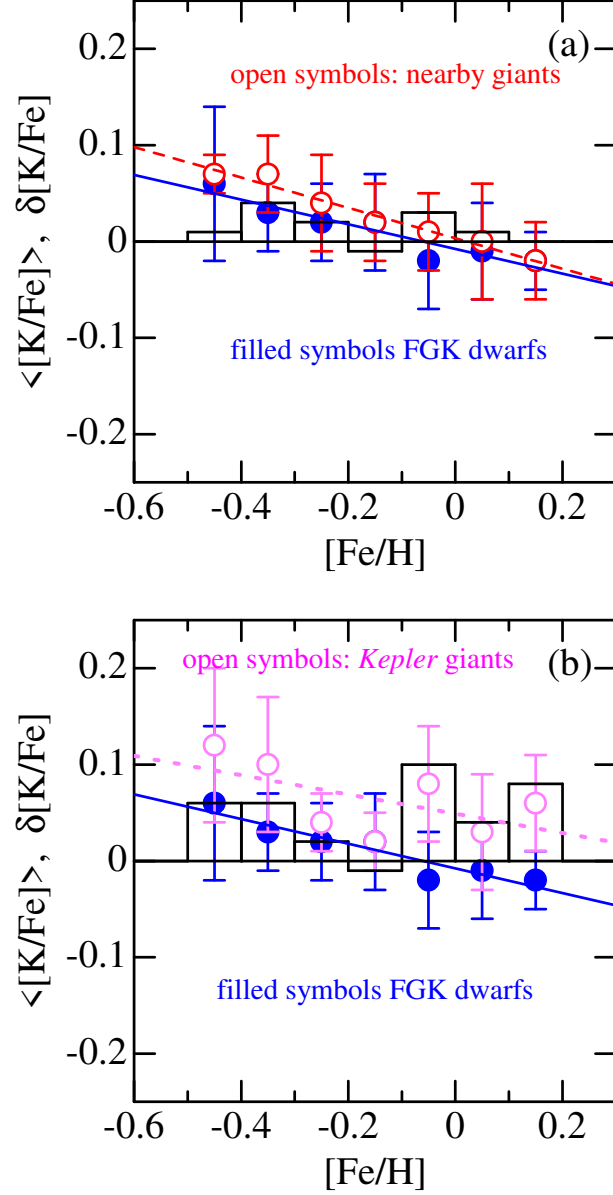
Fig. 8. The mean $\langle[K/Fe]\rangle$ values calculated at each metallicity group (0.1 dex bin within $-0.5 \leq [Fe/H] \leq +0.2$) are illustrated by symbols (attached error bars denote standard deviations), where filled and open circles correspond to dwarfs and giants, respectively. The bar graphs represent the giants$-$dwarfs differences ($\langle[K/Fe]\rangle_{giants} - \langle[K/Fe]\rangle_{dwarfs}$). The upper panel (a) shows the comparison of nearby giants vs. FGK dwarfs while the lower panel (b) is for *Kepler* giants vs. FGK dwarfs. The linear regression lines determined from these $\langle[K/Fe]\rangle$ values (cf. Section 5.2) are also drawn by solid, dashed, and dotted lines for FGK dwarfs, nearby giants, and *Kepler* giants, respectively.
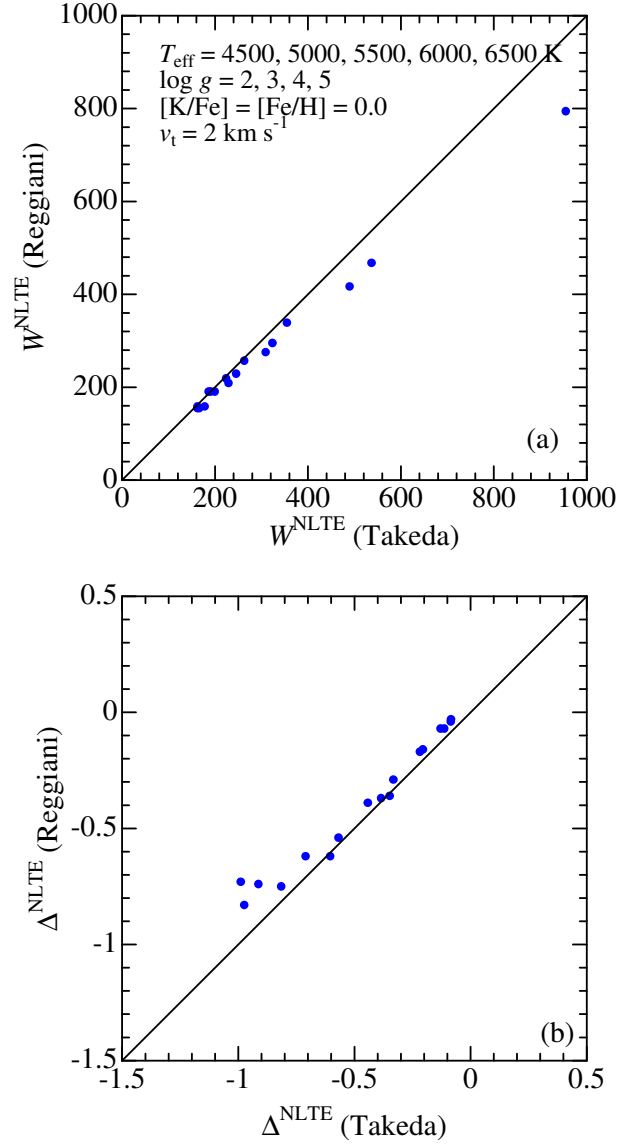
Fig. 9. Comparison of the non-LTE equivalent widths (W^{NLTE}: upper panel) and non-LTE corrections (Δ^{NLTE}: lower panel). In the ordinate are the values taken from Reggiani et al.'s (2019) non-LTE grid computed for the K I 7698.974 line by using the recent up-to-date atomic data, while those published by Takeda et al. (2002) are in the abscissa. Shown here are the cases of [K/Fe] = [Fe/H] = 0 and $v_{\mathrm{t}} = 2$ km s^{-1} with the combinations of ($T_{\mathrm{eff}} = 4500$, 5000, 5500, 6000, 6500 K) and ($\log g = 2$, 3, 4, and 5), for which direct comparisons are possible.